Egypt. J. Chem. **Vol. 66**, No. 8. pp. 439 - 448 (2023)

Egyptian Journal of Chemistry

http://ejchem.journals.ekb.eg/

Green Biosynthesized Selenium Nanoparticles and Bioactive Compounds by Gossypium barbadense L Extract and Their Cytotoxic Potential

Amani M.D. El-Mesallamy [a], Mohamed I.M. El-Zaidy[a], Mohamed El-Garby Younes[a], Sahar A.M Hussein[b]

[a] *Department of Chemistry, Faculty of Science, Zagazig University, Zagazig, 44519, Egypt.*
[b] *Department of Phytochemistry and Plant Systematics, Pharmaceutical Industries institute, National Research Centre, El Buhouth st. Dokki, Giza, 12622, Egypt*

Abstract

The aim of the work is to design green biosynthesized selenium nanoparticles mode to rapidly synthesize selenium nanoparticles (SeNPs) through *G. barbadense* leaves methanolic extract and confirming SeNPs synthesis by UV–visible spectroscopy. The methodologies applied for this work were field emission scanning electron microscopy with energy dispersive X-ray spectroscopy (FE-SEM-EDS) and high-resolution transmission electron microscopy (HR-TEM).

The LC-ESI-Mass analysis of *G. barbadense* leaves methanolic extract indicates the presence of 11 bioactive compounds, which they are capable of providing electrons for the reduction of selenium ions to SeNPs. This shielding layer can provide steric hindrance surrounding the particles, allowing them to be stabilized.

In addition to assess the anti-cancer efficacy of the SeNPs against the colorectal carcinoma "HCT116" and human pancreas epithelioid carcinoma "PANC1" using the MTT assay. As studies have shown that SeNPs biosynthesis downregulates the cancer cells when compared to normal doxorubicin drug. Markedly, The SeNPs had the most potent cytotoxic activity and HCT116 was more sensitive than PANC1. The IC_{50} of PANC1 cells were 358.54 ± 3.83 and 349.43 ± 7.76 while, IC_{50} values of HCT116 cells were 99.41 ± 1.87 and 240.79 ± 6.56 µg/mL for methanolic extract and SeNPs respectively, while the IC_{50} effect of Doxorubicin on HCT116 is 4.82±0.6 µg/mL and IC_{50} effect on PANC1 is 2.91±0.2 µg/mL.

Keywords: *selenium nanoparticles (SeNPs), Gossypium barbadense leaves, LC-ESI-Mass, Bioactive phenolic compounds, Cytotoxic Potential*

1. Introduction:

The use of plants for nanoparticle synthesis is preferable to microorganism because it removes the laborious procedure of keeping the cell in culture [1]. Due to the importance of selenium in human health, there has been a surge in interest in recent years [2]. Nanomaterials are of tremendous interest due to their unique physical, chemical, electrical, optical and thermal properties. Among the many types of nanomaterials, semiconductor nanoparticles are actively investigated due to their superior nonlinear characteristics, saturable absorption and optical biostability [3].

Nanoparticles can be synthesized biologically utilizing microorganisms and plant extracts. Biomolecules found in plant extracts such as polysaccharides, phenolic compounds, flavonoids, tannins, saponins, amino acids, enzymes, proteins and sugars are recognized to be potential selenium reducing agents with medical applications [4]. Because nanoparticles agglomerate, a stabilizer is frequently utilized to restrict their over-growth by covering with a single layer of polymer or surfactant, which decreases interactions between nanoparticles [5].

Selenium is essential for several main metabolic pathways, including thyroid hormone metabolism and immunological function. It also protects cells from

*Corresponding author e-mail: drsahar90@yahoo.com; (Sahar Awad Allah Hussein).
Received date 30 October 2022; revised date 21 November 2022; accepted date 24 November 2022
DOI: 10.21608/ejchem.2022.171646.7132

free radical damage incorporating into antioxidant enzymes. Se deficiency has been associated to several significant disorders, including cardiovascular disease, cancer and inflammatory diseases [6]. On the other hand, long-term Se supplementation or greater amounts may induce toxicity [7].

Selenium nanoparticles have a wide range of applications as well as numerous pharmacological properties such as Antileukemia activity of Avaram (Cassia auriculata) plant, Antioxidant and antimicrobial agent of Emblica officinalis plant, Antitumor activity towards HepG2 cells Chemotherapic agent for human liver cancer of Hawthorn plant, Antimicrobial activity against Proteus sp. of Ginger fruit, Antibacterial activity against Klebsiella pneumomiae and Bacillus subtillis. Of Ashwagandha plant, Inhibiting the breast-cancer cells (MCF-7) growth of Fenugreek plant, Cytotoxic effect against L6 cell lines of Java tea plant, Antibacterial and anti-fungal activity of Lavender leucas plant, antimicrobial activity against spoilage fungi and pathogenic bacteria strain of Aloe vera plant, Cytotoxicity against Vero cell of Garlic plant and Insecticidal agent against mosquito vectors of Clausena dentate plant [8].

One of the most important sources of synthesized SeNPs is G. barbadense. It is a perennial shrub, 1-3m tall, native to South America and now widely cultivated in the tropics, with a considerable presence in Egypt. It belongs to the genus Gossypium, family Malvaceae. In addition to being a cotton wool producing plant, its extracts have been discovered to have pharmacological value as an antibacterial, antihypertensive, antimalarial, antiulcer, aphrodisiac, and in promoting wound healing [9-11]. The phytochemicals in the G. barbadense leaves extract such as phenolic, flavonoids, glycosides, saponins, tannins and glycoside reported by Salako and Awodele [12] operate as reducing and capping agents responsible for the synthesis of Selenium nanoparticles (SeNPs).

2. Materials and Methods:

2.1. General.

All chemicals used are analytical grade and purchased from Sigma-Aldrich, the solvents used were purchased from Merck (Germany)

2.2. Plant Collection.

The *G. barbadense* leaves were collected in August 2021 from a natural field in Zagazig - Sharqia, Egypt and identified by Professor of Plant Taxonomy, Alaaeldin Sayed Ewase, Ministry of Environment. A voucher herbarium specimen (No. M145) was deposited in herbarium of National Research Center, (NRC), Giza, Egypt with global code (CAIRC).

*2.3. Extraction***.**

The leaves were washed several times with double distilled water and shade dried at room temperature. Aerial parts were finely grounded into a fine powder. The leaves powder (50 g) was defatted with petroleum ether 60-80^{o}, followed by n-hexane, finally by methanol by using Soxhlet apparatus. The crude extracts were concentrated till dryness. The extracts 6.58, 5.2, 3.91 gm, respectively, were stored at -4°C for further investigations.

2.4. Liquid Chromatography - Electrospray Ionization-Mass Spectrometry (LC-ESI-Mass).

The analysis was done at Drug Discovery and Development, Research Centre (Ain Shams University, Giza, Egypt) using an inverse stage C_{18} column (ACQUITY UPLCBEH C_{18} 1.7 µm particle size 2.1omb 5 mm Column)**,** to isolate phenolic acids and flavonoids of methanolic extract. The sample solution (100 µg/mL) was produced using MeOH grade solvent, filtered through a membrane disc filter (0.2 µm), and then submitted to LC-ESI-MS analysis. The sample quantities (10 µl) were injected into the fitted LC-ESI-MS instrument. The portable sample stage was prepared by filtering it with a 0.2 µm filter membrane disc and degassing it before injection with the sonication.

Gradient mobile phase elution was performed at a flow rate of 0.2 mL/min with two eluents: eluent A is H_2O acidified with 0.05% formic acid and eluent B is acetonitrile. The following parameters were used for analysis in negative ion mode: source temperature 150°C, cone voltage 30 eV, capillary voltage 3 kV, desolation temperature 440°C, cone gas flow 50 L/h and desolation gas flow 900L/h. Mass spectra were discovered utilizing the ESI negative ion mode between m/z 100–1000. Peaks and spectra were analyzed and provisionally identified using the Maslynx 4.1 software by comparing retention time (RT) with mass range and international data.

2.5. Biosynthesis of Selenium Nanoparticles.

Biogenic synthesis of SeNPs was carried out according to the method of Alam *et al.* [13] with slight adjustments. The synthesis was performed by adding 100 ml of diluted methanol extract (3mg stock extract/100ml distilled water) of *G. barbadense* leaves to 900 ml of freshly prepared aqueous sodium selenite (Na_2SeO_3) (10 mM) at 60° for 12 hours on a hot plate with a magnetic stirrer (1000 rpm). The SeNPs were isolated and purified by centrifugation at 8000 rpm for 20 minutes, followed by redispersion of the nanoparticle pellet in acetone. The pure nanoparticles were kept at 4°C for analysis after air drying.

2.6. Characterization of Selenium Nanoparticles

The SeNPs initially analyzed by using a digital pH meter (Eutech Cybersacn pH 300). Then the Rigol ultra-3660 UV-vis spectroscopy within the range 200–800 nm. Subsequently, FESEM was used to examine the morphology, scale and surface area of the SeNPs. The SeNPs solutions were ultrasonicated for 15 minutes at room temperature, and one drop of the sample was put on a glass slide. After drying, the glass slide was coated with gold and analyzed under a Field Emission Scanning Electron Microscope (Zeiss Evo-MA 10, Germany). Se nano powder was suspended in ethanol, sonicated then coated onto a copper grid and allowed to dry and examined by JEOL-2100 HR-TEM.

2.7. Cytotoxic Activity

Cancer cell lines (human colon epithelial colorectal carcinoma "HCT" and human pancreas epithelial epithelioid carcinoma "PANC1") were procured from tissue culture Lab in Science Way for Scientific Researches, Nasr City, Cairo, Egypt. To evaluate the cytotoxicity of the methanolic extract and SeNPs, The MTT assay involves the conversion of the water-soluble yellow dye MTT [3- (4,5-dimethylthiazol-2-yl)-2,5-diphenyltetrazolium bromide] to an insoluble purple formazan by the action of mitochondrial reductase, it was performed in 96-well plates [14,15]. The whole procedure was maintained under sterile conditions *via* the use of a laminar air-flow cabinet, following culturing and sub-culturing technique adopted by Alley *et al*. [16].

*2.8. Statistical Analysis***.**

The data were statistically analyzed using the Statistical Package for the Social Sciences, SPSS version 23 (Copyrighted by IBM SPSS software, USA). The data were presented as a mean ± standard error of mean (SEM).

3. Results and Discussion

3.1. LC-ESI-Mass analysis.

The analysis of MeOH extract of *G. barbadense* indicate the presence of 11 major phenolic compounds; kaempferol, quercetin-3-*O*-pentoside, kaempferol-3-sulfate , quercetin-3-*O*-β-glucoside,quercetin-3-*O*-(6-acetyl-β-glucoside), kaempferol-3-*O*-glucuronide, epigallocatechin gallate , aspalathin, kaempferol-3,7,4'-trimethyl ether, isorhamnetin-3-*O*-glucuronide and protocatechuic acid-3-*O*-glucoside were recorded at (Fig.1& Table 1) that might have been responsible for their therapeutic potential.

Biosynthesis of SeNPs by *G. barbadense* leaves extract is due to the presence of a high number of bioactive phenolic compounds are shown in (Fig.2), capable of providing electrons for the reduction of selenium ions to SeNPs. During the process, the carboxyl and hydroxyl groups produce a protective coating on the surface of the Selenium nanoparticles as shown in (Fig.3). This shielding layer can provide steric hindrance surrounding the particles, allowing them to be stabilized [17,18].

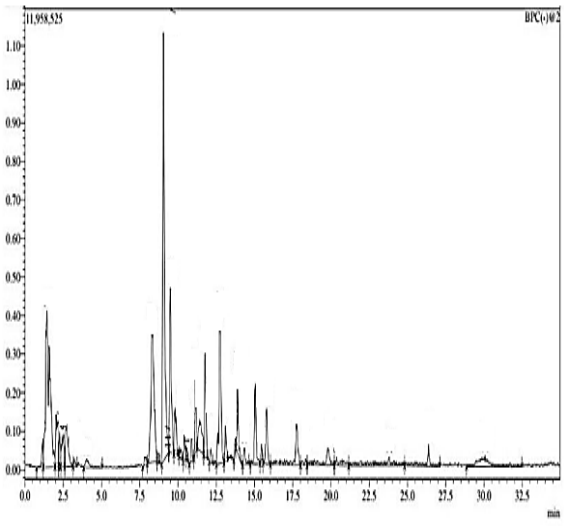

Figure1. LC-ESI-Mass, profile of *G. barbadense* leaves MeOH extract

Table 1. Bioactive phenolic compounds identified by LC-ESI-Mass of *G. barbadense* leaves extract

Peak No.	$R_{t\ (min)}$	Conc. (%)	Base Peak m/z	Exact Mass (g/mol)	Chemical formula	Identification Compounds
1	2.52	11.7	285.10	286.23901	$C_{15}H_{10}O_6$	Kaempferol
2	7.83	8.9	433.10	434.08490	$C_{20}H_{18}O_{11}$	Quercetin -3-*O*-Pentoside
3	8.31	14.9	365.10	366.17053	$C_{15}H_{10}O_9S$	Kaempferol- 3-Sulfate
4	9.04	8.4	463.15	464.37900	$C_{21}H_{20}O_{12}$	Quercetin-3-*O*-β-glucoside
5	9.49	7.5	505.10	506.10605	$C_{23}H_{22}O_{13}$	Quercetin-3-*O* -(6-acetyl-β-glucoside)
6	10.42	5.9	461.30	462.07983	$C_{21}H_{18}O_{12}$	Kaempferol-3-*O*-glucuronide
7	11.77	6.6	457.25	458.08490	$C_{22}H_{18}O_{11}$	Epigallocatechin gallate
8	12.73	9.7	451.20	452.13190	$C_{21}H_{24}O_{11}$	Aspalathin
9	13.89	5.6	327.30	328.09470	$C_{18}H_{16}O_6$	Kaempferol-3,7,4'-trimethyl ether
10	15.78	7.7	491.20	492.38901	$C_{22}H_{20}O_{13}$	Isorhamnetin-3-*O*-glucuronide
11	19.80	10.2	315.15	316.26501	$C_{13}H_{16}O_9$	Protocatechuic acid-3-*O*-glucoside

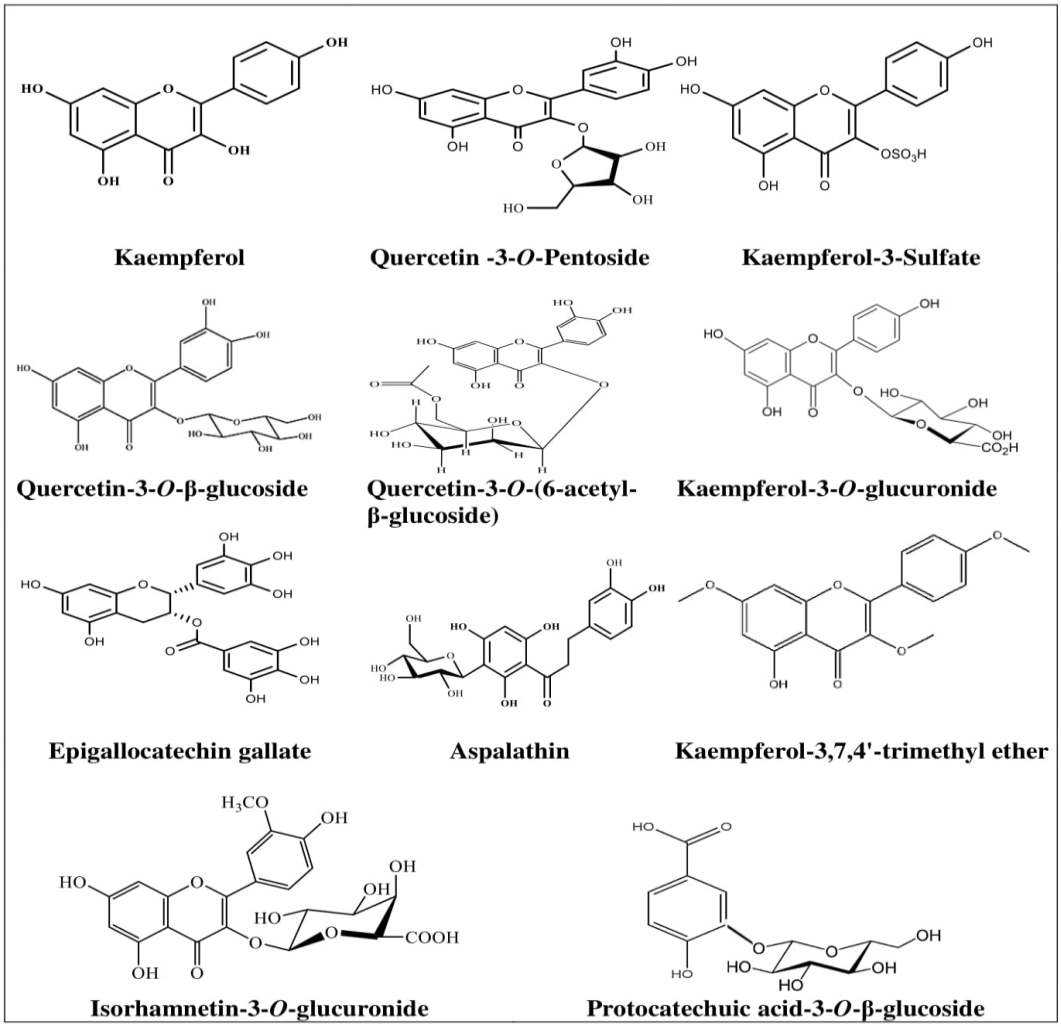

Figure2. Chemical structures of bioactive phenolic compounds in *G. barbadense* leaves MeOH extract

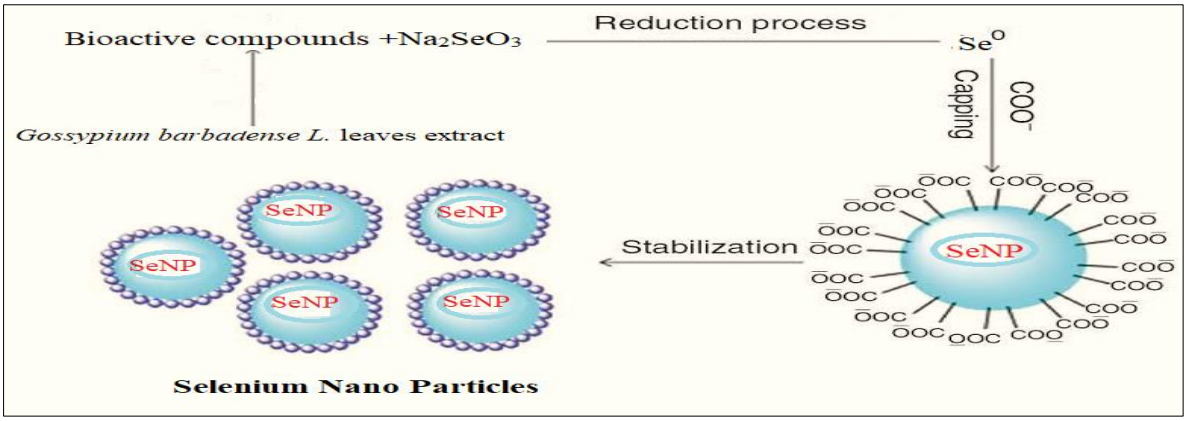

Figure3. Mechanism of synthesis of Selenium Nanoparticles

3.2. Characterization of green synthesized SeNPs.

Change in Visual Color. The first sign of SeNPs production is a change in the hue of the reaction mixture. The colour shifted from light yellow to brick red, indicating the creation of Selenium nanoparticles as shown in (Fig.4-a). A similar visual observation was made in Se NPs synthesized using aqueous extract of garlic (Allium sativum) clove [19].

3.3. Reduction Of pH in Reaction

In the presence of *G. barbadense* leaves extract, the pH of the reaction mixture reduced from 8.04 to 5.28, indicating a reduction of 10mM (Na_2SeO_3) during the synthesis of selenium nanoparticles. This finding was agreed with the involvement of *Mangifera Indica L.* (Musk) peels extract, which lowered pH during the biogenic creation of silver nanoparticles [20].

The hue of the Na_2SeO_3 solution changed from bright yellow to brick red when the initial pH of the solution was reduced. This might be because the dissociation condition for capping functional groups in *G. barbadense* leaves extract is affected by the pH of the reaction solution. The higher pH aids in the deprotonation of the capping functional groups. Deprotonated functional groups may be more negatively charged. As a result of the electrostatic repulsion, the negatively charged groups bond to the SeNPs and increase their stability [21].

3.4. U.V - visible spectrophotometric analysis.

The formation of SeNPs was initially confirmed by UV-vis spectroscopy within the range 200–800 nm. The absorption spectrum of green synthesized SeNPs showed a characteristic peak at 275 to 280 nm (Fig.4b). The optical absorption spectra of metal nanoparticles is dominated by surface plasmon resonance (SPR), which varies with particle size, shape, aggregation state and dielectric medium [22]. The size of the SeNPs was found to be connected to the nature of the UV-visible spectra, and if the particle size is 100nm or larger, it exhibits obvious regular maxima (kmax) in the visible region [23]. As a result, the current spectra for SeNPs indicated a size of roughly 20 nm. Because of the existence of suitable (SPR), the peaks near spectra at 275 nm, the methanolic extract of G. barbadense leaves was able to synthesis SeNPs. The peaks in various time intervals are about 275 nm, demonstrating the stability and regularity of SeNPs. The peak location does not vary with time, but the difference in maximum absorbance with increasing time suggests that the rate of selenium nanoparticle formation is rising. SeNPs produced from Calendula officinalis extract showed distinct absorption bands at 265 nm [24]. Furthermore, the absorption spectra of SeNPs produced using garlic (Allium sativum) clove extract shows distinct absorption bands at 267-367 nm.

3.5. Field Emission Scanning Electron Microscopy (FESEM).

SEM images show SeNPs generated by G. barbadense leaves extract have a relatively spherical shape as shown in (Fig.4-c). Interactions between biomolecules coated with Se0 through hydrogen bonds resulted in the formation of selenium nanoparticles. This observation is analogous to the fact that Spherical SeNPs were produced utilizing an aqueous extract of the Horseshoe geranium plant [25]. SeNPs produced from Catharanthus roseus extract were also spherical [26].

3.6. High-Resolution Transmission Electron Microscopy (HR-TEM) Analysis.

TEM examination may be utilized to investigate the crystalline properties and size of the synthesized NPs. The JEOL-2100 was used for the analysis and the images at various magnifications are exhibited in (Fig.4-d). TEM images displaying the major series of particle size that were between 1.17 to 3.18 nm. This observation is consistent with the size of the produced SeNPs, which were in the 10-80nm range utilizing Arauna aqueous extract and were spherical [27]. Furthermore, spherical selenium nanoparticles with an average size of 4-16 nm were produced from a Mountain persimmon extract [28]. The selected area electron diffraction (SAED) pattern of SeNPs produced by G. barbadense leaves extract is shown in (Fig.4-e). The typical SAED pattern, with brilliant circular rings that revealed the extremely crystalline nature of green produced SeNPs.

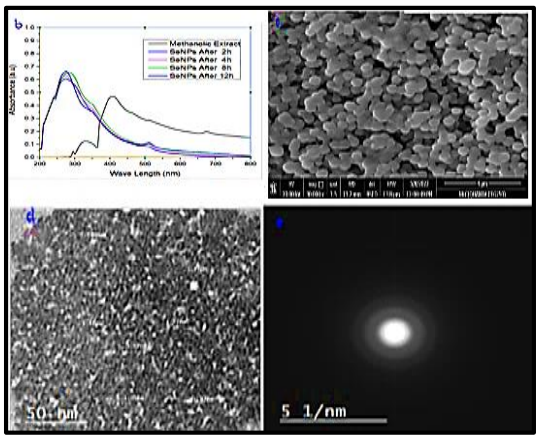

Figure4. Schematic illustration of characterization of green synthesized SeNPs
(b) U.V. spectrophotometric analysis at different time during production of SeNPs
(c) FESEM images of SeNPs
(d) TEM images of SeNPs
(e) SAED Images of SeNPs

3.7. Cytotoxic assay.

The cytotoxicity of the examined materials (G. barbadense leaves extract and SeNPs) was investigated using Doxorubicin as a positive control and the untreated cells were the negative control.

From the MTT assay findings present in (Fig. 5), both the plant extract and SeNPs showed a significant selective cytotoxic impact on the HCT116 and PANC1 cancer cell lines.

This effect was dose-dependent, where 1000 µg/ml had a larger effect than 31.25 µg/mL and so on.

Furthermore, the level of cytotoxicity was clearly controlled by cell type and the material used. Markedly the SeNPs had the most potent cytotoxic activity and HCT116 was more sensitive than PANC1, as shown in (Fig.5). IC50 of PANC1 cells were 358.54 ± 3.83 and 349.43 ± 7.76 while, IC50 values of HCT116 cells were 99.41 ± 1.87 and 240.79 ± 6.56 µg/mL for the extract and SeNPs respectively, while the IC50 effect of Doxorubicin on HCT116 is 4.82±0.6 µg/mL and IC50 effect on PANC1 is 2.91±0.2 µg/mL. This is consistent with evidence from microscopic examinations, which revealed that cytotoxic activity may be identified by membrane blebbing, cell enlargement or shrinkage, nuclear margination or fragmentation, and chromatin condensation (Fig.6).

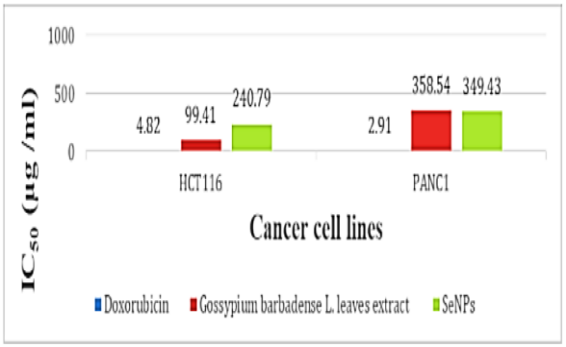

Figure5. IC50 of G. barbadense L. leaves MeOH extract, SeNPs and Doxorubicin on the HCT116 and PANC1 cancer cells

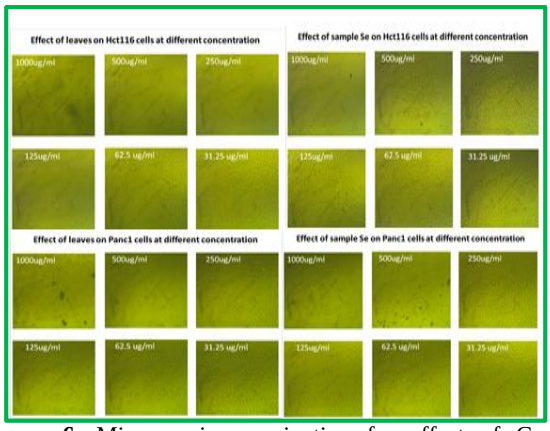

Figure 6. Microscopic examination for effect of G. barbadense L. leaves Methanolic extract, SeNPs and Doxorubicin on the HCT116 and PANC1 cancer cells.

The malignant condition of excessive cell multiplication considered the second leading cause of death in the world. Between various cancer types, colorectal and pancreas cancers are the most dangerous and being associated with highest fatality [29]. One of the most difficult aspects in modern scientific study is developing new. Herbal plants and plant-derived medicines have long been employed in ancient communities across the world as a source of potent anticancer agents, and they are gaining appeal in modern society [30]. As a result of their numerous adverse effects, expensive cost and higher risk of recurrence, synthetic medications are becoming less frequent [31]. One of the goals of this work was to compare the cytotoxic effects of *G. barbadense*. leaves extract and SeNPs against (HCT116) colon cancer cell line and (PANC1) pancreatic cancer cell line using the MTT protocol. It is well documented that lowering of particle size increases their functionality as anticancer and antimicrobial agent due to the larger surface to volume ratio. Indeed, our data reveal that SeNPs have a cytotoxic effect on cancer cell lines such as colon (HCT116) and pancreatic (PANC1), where the cytotoxicity of SeNPs dependent on dose, concentration, duration, and particle size. The synthesized SeNPs showed decreased % cell viability against colon (HCT116) and pancreatic (PANC1) cell lines, but SeNPs have less cytotoxic effects against colon (HCT116) cell line than methanolic extract of G. barbadense L. leaves, while the leaves extract and SeNPs have similar cytotoxic activities against pancreatic (PANC1) cell line. This is due to bioactive metabolites borne on the surface of SeNPs, which are responsible for anticancer actions. The high flavonoid and phenolic content of G. barbadense L. leaves extract can be linked to its cytotoxic effect. In animal studies, flavonoids inhibit cancer cell proliferation and tumor development. The pattern of hydroxylation of the flavanone and flavone B rings appears to be important for their actions, particularly protein kinase inhibition and antiproliferation [32]. Biosynthesized SeNPs have been employed in a variety of applications, including medicine, agriculture, and industry, due to their low toxicity and environmental friendliness. Several studies have verified the anticancer impact of SeNPs derived from green synthesis [33]. The cytotoxicity of SeNPs varies depending on the method employed to create the nanomaterial. Various mechanisms for Se anticancer action have been proposed, including cell cycle arrest, antioxidation, apoptosis, and disruption of cell signalling pathways, and there is a large body of literature on this issue [34- 38]. SeNPs can operate as a carrier for chemotherapeutic medications, carrying them to the target side, accumulating selectively inside malignant cells and causing reactive oxygen species production [39]. In a mouse model, the synthesis of these reactive species was more efficient than Se (IV), resulting in powerful therapeutic effects and a viable technique for cancer therapy. Kumari et al. [40], found that Se-CurNPs were more effective against colorectal carcinoma cells (HCT116) than other cancer cell lines and had pleiotropic anticancer effects.

Additionally, Huang et al. [41], stated that exhibits the great efficacy of functionalized SeNPs for colorectal cancer treatment and highlights the critical role of autophagy in triggering apoptosis and cell cycle arrest to cause cell death. Furthermore, Hussain et al. [42]. demonstrated that biosynthesized Selenium (Se), Silver Selenium (AgSe) nanoparticles derived from Litchi chinensis (Sonn) seed demonstrated broad-spectrum anticancer activity with PTT therapy, implying that they promote ROS generation by modulating mitochondrial apoptosis induction in PANC-1 cancer cells.

Furthermore, combining SeNPs with doxorubicin (a chemotherapy treatment used to treat cancer) increased the cytotoxic impact.

4. Conclusion

In the current study, from the best of our knowledge, no published studies have investigated using an alcoholic extract of G. barbadense L. leaves against the cancer cell lines (HCT116and PANC1). We generated SeNPs from the alcoholic leaves extract of the plant rich with bioactive phenolic compounds were demonstrated using LC-ESI-MS analysis. As a result, the bioactive compounds in the extract served as a reducing and stabilizing factor in the production of SeNPs.

Different techniques were used to authenticate the Selenium nanoparticles “pH analysis, UV–vis, FESEM and HR-TEM” that confirmed the presence of Selenium nanoparticles with an average size of 1-3 nm. Both the alcoholic extract of G. barbadense L. leaves and the synthesized Selenium nanoparticles showed an attractive selective cytotoxic action against two cancer lines examined, providing

satisfying 'safer and cheaper' alternatives to traditional therapeutic regimens. With all their promising properties of green synthesized SeNPs, further biological activities should be investigated. Moreover, the findings of the current study need to be validated by evaluating these materials for in vivo application.

5. References:

1. Manna, L., Scher, E. C., & Alivisatos, A. P. Synthesis of soluble and processable rod, arrow, teardrop-, and tetrapod-shaped CdSe nanocrystals. Journal of the American Chemical Society, 122 (51), 12700-12706 (2000).
2. Ren, F., He, X., Wang, K., & Yin, J. Biosynthesis of gold nanoparticles using catclaw buttercup (Radix Ranunculi Ternati) and evaluation of its colloidal stability. Journal of Biomedical Nanotechnology, 8 (4), 586-593(2012).
3. Rayman, M. P. Selenium intake, status, and health: A complex relationship. Hormones, 19 (1), 9-14 (2020)
4. Kieliszek, M., & Błażejak, S. Current knowledge on the importance of selenium in food for living organisms: a review. Molecules, 21(5), 609 (2016).
5. Boroumand, S., Safari, M., Shaabani, E., Shirzad, M., & Faridi-Majidi, R.Selenium nanoparticles: synthesis, characterization and study of their cytotoxicity, antioxidant and antibacterial activity. Materials Research Express, 6(8), 0850d8 (2019).
6. Misra, S., Boylan, M., Selvam, A., Spallholz, J. E., & Björnstedt, M. Redox-active selenium compounds from toxicity and cell death to cancer treatment. Nutrients, 7(5), 3536-3556 (2015).
7. Rayman, M. P., Winther, K. H., Pastor-Barriuso, R., Cold, F., Thvilum, M., Stranges, S.& Cold, S. Effect of long-term selenium supplementation on mortality: results from a multiple-dose, randomised controlled trial. Free Radical Biology and Medicine, 127, 46-54 (2018).
8. Pyrzynska, K., & Sentkowska, A. Biosynthesis of selenium nanoparticles using plant extracts. Journal of Nanostructure in Chemistry, 1-14 (2021).
9. Emmanuel, E. E., Sherifat, O. A., & Isiaka, A. O. Constituents and antimicrobial properties of the leaf essential oil of G. barbadense (Linn.). Journal of Medicinal Plants Research, 5(5), 702-705 (2011).
10. Ejelonu, O.C., Elekofehinti, O.O., Borisade, O., Olaleye, M.T. Possible in vitro antioxidant potential of G. barbadense eaf aqueous extract and its effect on lipid profile and liver enzymes of albino rats. Res. J. Pharmaceut. Biol.Chem. Sci. 5, 129–136(2014).
11. Ikobi, E., Igwilo, C. I., Azubuike, C. P., & Awodele, O. Antibacterial and wound healing properties of methanolic extract of dried fresh G. barbadense leaves. Asian J. Biomed. Pharmaceut. Sci. 2, 32–37(2012).
12. Salako, O. A., & Awodele, O. Evaluation of the antimalarial activity of the aqueous leaf extract of G. barbadense (Malvaeceae) in mice. Drugs and Therapy Studies, 2(1), e2-e2 (2012).
13. Alam, H., Khatoon, N., Raza, M., Ghosh, P. C., & Sardar, M. Synthesis and characterization of nano selenium using plant biomolecules and their potential applications. BioNanoScience, 9(1), 96-104(2019).
14. Slater, T. F., Sawyer, B., & Sträuli, U. Studies on succinate-tetrazolium reductase systems: III. Points of coupling of four different tetrazolium salts III. Points of coupling of four different tetrazolium salts. Biochimica et biophysica acta, 77, 383-393(1963).
15. Van de Loosdrecht, A. A., Beelen, R. H. J., Ossenkoppele, G., Broekhoven, M. G., & Langenhuijsen, M. M. A. C. A tetrazolium-based colorimetric MTT assay to quantitate human monocyte mediated cytotoxicity against leukemic cells from cell lines and patients with acute myeloid leukemia. Journal of immunological methods, 174(1-2), 311-320(1994).
16. Alley, M. C., Scudiero, D. A., Monks, A., Hursey, M. L., Czerwinski, M. J., Fine, D. L.,& Boyd, M. R. Feasibility of drug screening with panels of human tumor cell lines using a microculture tetrazolium assay. Cancer research, 48(3), 589-601(1988).
17. Bartosiak, M., Giersz, J., & Jankowski, K. Analytical monitoring of selenium nanoparticles green synthesis using photochemical vapor generation coupled with MIP-OES and UV–Vis

spectrophotometry. Microchemical Journal, 145, 1169-1175(2019).
18. Ingole, A. R., Thakare, S. R., Khati, N. T., Wankhade, A. V., & Burghate, D. K. Green synthesis of selenium nanoparticles under ambient condition. Chalcogenide Lett, 7(7), 485-489(2010).
19. Satgurunathan, T., Bhavan, P. S., & Komathi, S. Green synthesis of selenium nanoparticles from sodium selenite using garlic extract and its enrichment on Artemia nauplii to feed the freshwater prawn Macrobrachium rosenbergii post-larvae. Res J Chem Environ, 21(10), 1-12(2017).
20. Elmesallamy, A., El-zaidy, M., Sahar A.M.Hussein, Green Synthesis of Silver Nanoparticles Using Mangifera Indica L. (Musk) Peels Extract and Evaluation of Its Cytotoxic Activities. Egyptian Journal of Chemistry, 65(7), 1-6(2022).
21. Yang, N., & Li, W. H. Mango peel extract mediated novel route for synthesis of silver nanoparticles and antibacterial application of silver nanoparticles loaded onto non-woven fabrics. Industrial Crops and Products, 48, 81-88(2013).
22. Mulvaney, P. Surface plasmon spectroscopy of nanosized metal particles. Langmuir, 12(3), 788-800(1996).
23. Lin, Z. H., & Wang, C. C. Evidence on the size-dependent absorption spectral evolution of selenium nanoparticles. Materials Chemistry and Physics, 92(2-3), 591-594(2005).
24. Hernández-Díaz, J. A., Garza-García, J. J., León-Morales, J. M., Zamudio-Ojeda, A., Arratia-Quijada, J., Velázquez-Juárez, G.,& García-Morales, S. Antibacterial activity of biosynthesized selenium nanoparticles using extracts of calendula officinalis against potentially clinical bacterial strains. Molecules, 26(19), 5929(2021).
25. Fardsadegh, B., Vaghari, H., Mohammad-Jafari, R., Najian, Y., & Jafarizadeh-Malmiri, H. Biosynthesis, characterization and antimicrobial activities assessment of fabricated selenium nanoparticles using Pelargonium zonale leaf extract. Green Processing and Synthesis, 8(1), 191-198(2019).
26. Deepa, B., & Ganesan, V. Bioinspiredsynthesis of selenium nanoparticles using flowers of Catharanthus roseus (L.) G. Don. and Peltophorum pterocarpum (DC.) Backer ex Heyne–a comparison. Int J Chem Technol Res, 7, 725-733(2015).
27. Prasad, K. S., & Selvaraj, K. Biogenic synthesis of selenium nanoparticles and their effect on As (III)-induced toxicity on human lymphocytes. Biological trace element research, 157(3), 275-283(2014).
28. Kokila, K., Elavarasan, N., & Sujatha, V. Diospyros montana leaf extract-mediated synthesis of selenium nanoparticles and their biological applications. New Journal of Chemistry, 41(15), 7481-7490(2017).
29. WHO. World Health Organization. Geneva, Switzerland, – The International Agency for Research on Cancer (IARC) 12 September 2018. http://gco.iarc.fr/tomorrow/home (2018).
30. George, N. M., Abdelhaliem, E., & Abdel-Haleem, M. GC-MS Identification of Bioactive Compounds in Unripe Solanum nigrum Berries and Assessment of Antioxidant and Anticancer Activities. latin american journal of pharmacy, 40(11), 2702- 2708 (2021).
31. Pande, J., & Chanda, S. Screening of anticancer properties of some medicinal plants-review. Int J Curr Microbiol Appl Sci, 9(3), 1348-1362(2020).
32. Kanadaswami C., Lee L., Lee P.H., Hwang J., Ke F., Huang Y. and Lee M. The antitumor activities of flavonoids. In vivo, 19 (5): 895-909(2005).
33. Ezhuthupurakkal, P. B., Polaki, L. R., Suyavaran, A., Subastri, A., Sujatha, V., & Thirunavukkarasu, C. Selenium nanoparticles synthesized in aqueous extract of Allium sativum perturbs the structural integrity of Calf thymus DNA through intercalation and groove binding. Materials Science and Engineering: C, 74, 597-608(2017).
34. Kumar, A., & Prasad, K. S. Role of nano-selenium in health and environment. Journal of Biotechnology, 325, 152-163(2021).
35. Khurana, A., Tekula, S., Saifi, M. A., Venkatesh, P., & Godugu, C. Therapeutic applications of selenium nanoparticles. Biomedicine & Pharmacotherapy, 111, 802-812(2019).
36. Kondaparthi, P., Flora, S. J. S., & Naqvi, S. Selenium nanoparticles: An insight on its Pro-oxidant and antioxidant properties. Front. Nanosci. Nanotechnol, 6, 1-5(2019).

37. Wallenberg, M., Misra, S., & Björnstedt, M. Selenium cytotoxicity in cancer. Basic & clinical pharmacology & toxicology, 114(5), 377-386(2014).
38. Huang, Y., He, L., Liu, W., Fan, C., Zheng, W., Wong, Y. S., & Chen, T. Selective cellular uptake and induction of apoptosis of cancer-targeted selenium nanoparticles. Biomaterials, 34(29), 7106-7116(2013).
39. Zhao, G., Wu, X., Chen, P., Zhang, L., Yang, C. S., & Zhang, J. Selenium nanoparticles are more efficient than sodium selenite in producing reactive oxygen species and hyper-accumulation of selenium nanoparticles in cancer cells generates potent therapeutic effects. Free Radical Biology and Medicine, 126, 55-66(2018).
40. Kumari, M., Ray, L., Purohit, M. P., Patnaik, S., Pant, A. B., Shukla, Y., ... & Gupta, K. C. Curcumin loading potentiates the chemotherapeutic efficacy of selenium nanoparticles in HCT116 cells and Ehrlich's ascites carcinoma bearing mice. European Journal of Pharmaceutics and Biopharmaceutics, 117, 346-362(2017).
41. Huang, G., Liu, Z., He, L., Luk, K. H., Cheung, S. T., Wong, K. H., & Chen, T. Autophagy is an important action mode for functionalized selenium nanoparticles to exhibit anti-colorectal cancer activity. Biomaterials science, 6(9), 2508-2517(2018).
42. Hussain, A. Plasmonic photothermal effect on cytotoxicity of biogenic nanostructure synthesized through Litchi chinensis Sonn. Inorganic and Nano-Metal Chemistry, 1-13(2021).